Journal of Applied Physics

Thermoelastic properties of tungsten at simultaneous high pressure and temperature

Cite as: J. Appl. Phys. **128**, 105105 (2020); https://doi.org/10.1063/5.0022536
Submitted: 21 July 2020 . Accepted: 22 August 2020 . Published Online: 09 September 2020

Xintong Qi, Nao Cai, Siheng Wang, and Baosheng Li

Journal of Applied Physics ARTICLE scitation.org/journal/jap

Thermoelastic properties of tungsten at simultaneous high pressure and temperature

Cite as: J. Appl. Phys. **128**, 105105 (2020); doi: 10.1063/5.0022536
Submitted: 21 July 2020 · Accepted: 22 August 2020 ·
Published Online: 9 September 2020

View Online Export Citation CrossMark

Xintong Qi,[1,2,a)] Nao Cai,[2,b)] Siheng Wang,[1] and Baosheng Li[1,2]

AFFILIATIONS

[1]Department of Geosciences, Stony Brook University, Stony Brook, New York 11794, USA
[2]Mineral Physics Institute, Stony Brook University, Stony Brook, New York 11794, USA

[a)]**Author to whom correspondence should be addressed:** xintong.qi@stonybrook.edu
[b)]**Current address:** University of Chinese Academy of Sciences, No. 19(A) Yuquan Road, Shijingshan District, Beijing 100049, People's Republic of China

ABSTRACT

The compressional (P) and shear wave velocities (S) and unit cell volumes (densities) of polycrystalline tungsten (W) have been measured simultaneously up to 10.5 GPa and 1073 K using ultrasonic interferometry in conjunction with x-ray diffraction and x-radiography techniques. Thermoelastic properties of W were derived using different methods. We obtained the isothermal bulk modulus $K_{T0} = 310.3$ (1.5) GPa, its pressure derivative $K'_{T0} = 4.4(3)$, its temperature derivative at constant pressure $(\partial K_T/\partial T)_P = -0.0138(1)$ GPa K^{-1} and at constant volume $(\partial K_T/\partial T)_V = -0.0050$ GPa K^{-1}, the thermal expansion $\alpha(0, T) = 1.02(27) \times 10^{-5} + 7.39(3.2) \times 10^{-9}\, T$ (K^{-1}), as well as the pressure derivative of thermal expansion $(\partial\alpha/\partial P)_T = -1.44(1) \times 10^{-7}$ K^{-1}GPa^{-1} based on the high-temperature Birch–Murnaghan equation of state (EOS), the Vinet EOS, and thermal pressure approach. Finite strain analysis allowed us to derive the elastic properties and their pressure/temperature derivatives independent of the choice of pressure scale. A least-squares fitting yielded $K_{S0} = 314.5(2.5)$ GPa, $K_{S0}' = 4.45(9)$, $(\partial K_S/\partial T)_P = -0.0076(6)$ GPa K^{-1}, $G_0 = 162.4(9)$ GPa, $G_0' = 1.8(1)$, $(\partial G/\partial T)_P = -0.0175(9)$ GPa K^{-1}, and $\alpha_{298K} = 1.23 \times 10^{-5}$ K^{-1}. Fitting current data to the Mie–Grüneisen–Debye EOS with derived $\theta_0 = 383.4$ K yielded $\gamma_0 = 1.81(6)$ and $q = 0.3$. The thermoelastic parameters obtained from various approaches are consistent with one another and comparable with previous results within uncertainties. Our current study provides a complete and self-consistent dataset for the thermoelastic properties of tungsten at high P–T conditions, which is important to improve the theoretical modeling of these materials under dynamic conditions.

INTRODUCTION

The diamond anvil cell (DAC) and multi-anvil large volume presses are the two most commonly utilized techniques to generate static high pressures for experimental studies on the structural, physical, and chemical properties of materials in response to stress. Accurate determination of pressures in these experiments is needed for comparison between experimental results and theoretical calculations, thus the validity of the predictive model can be evaluated. Certain experimentally measurable properties of candidate pressure scale materials need to be well-determined as functions of pressure, such as the equations of state (EOS). Various EOS formulations for solids at high pressures have been developed and comprehensive reviews of these EOS are available in the literature (e.g., Refs. 1–3), among which the Birch EOS[1] and the Vinet EOS[2] are the most-used formulations to derive thermodynamic parameters. Previous EOS of metals have been studied up to Mbar conditions (e.g., Refs. 3 and 4), however, most were limited to room temperature. Thermoelastic properties for metals still need to be investigated under simultaneous high pressure and temperature conditions.

5d transition metal tungsten (W) features the highest melting point of all non-alloyed metals and very high moduli of elasticity. Materials strength and resistance to wear and corrosion can be greatly increased by alloying with tungsten. Because of these unique properties, tungsten and its alloys have been widely used for military, aerospace, electronics, and other applications.[5] Tungsten crystallizes in a body-centered-cubic (bcc) structure at ambient conditions. The stability of the bcc phase spans a wide range in pressure and temperature,[6–9] making tungsten an excellent pressure calibrant in diamond anvil cell high-pressure experiments. Several experimental and theoretical studies have been carried out

to investigate the elastic properties and EOS of tungsten, including ultrasonic measurements,[10–13] shock wave experiments,[14] and static compression.[15–18] However, most previous works were carried out at high pressures and room temperature or at high temperatures and room pressure. Up to now, only two sets of EOS data of W at simultaneous high pressures and high temperatures were reported by Dubrovinsky *et al.*[16] up to 46.6 GPa, 2100 K and Litasov *et al.*[17] up to 33.5 GPa and 1673 K, respectively. Meanwhile, results on the shear properties of W as a function of pressure and/or temperature are still rare. In this study, we conducted sound velocity measurements on polycrystalline tungsten at simultaneous high P–T conditions using ultrasonic interferometry in conjunction with synchrotron x-ray diffraction techniques up to 10.5 GPa and 1073 K. Compressional (P) and shear (S) wave velocities as well as the unit-cell volumes (densities) were presented. The elastic bulk and shear moduli, their pressure and temperature derivatives and pressure derivative of thermal expansion were derived by different approaches. The present study offers a comprehensive dataset for the thermoelasticity of polycrystalline bcc W, which is crucial for modeling its behavior under static and dynamic conditions.

METHOD

The polycrystalline tungsten sample used for acoustic measurement was hot-pressed at 5 GPa and 1373 K for 1.5 h in a 2000-ton uniaxial split-cylinder apparatus (USCA-2000) in the High Pressure Laboratory at Stony Brook University using fine-grained tungsten powder (Sigma Aldrich, $\geq$ 99.99%) as the starting material. The recovered sample was well sintered with a bulk density of 19.260(2) g/cm^3 measured by the Archimedes' immersion method. The result is essentially identical to the theoretical value of 19.256(26) g/cm^3,[18] indicating a high-quality and crack-free specimen that is ideal for the subsequent ultrasonic experiments. More details about the sintering experimental setup can be found in Ref. 19

High-pressure and high-temperature ultrasonic experiments were conducted up to 10.5 GPa and 1073 K in a 1000-ton Kawai-type, multi-anvil apparatus (T-25) in conjunction with *in situ* x-ray diffraction at beamline 13-ID-D of GSECARS, Advanced Photon Source, Argonne National Laboratory. Details of the experimental setup can be found elsewhere.[20] Figure 1(a) shows the schematic diagram of the octahedral cell assembly. A dual-mode piezoelectric $LiNbO_3$ transducer (50 MHz resonant frequency for P waves and 30 MHz for S waves) was used to generate and receive acoustic signals simultaneously. The sample sit roughly in the center of the cell. MgO octahedron was used as the pressure-transmitting medium and graphite was used as a furnace material. One side of the sample was in direct contact with a dense polycrystalline alumina that served as a buffer rod, while the other end was backed by a disk of NaCl + BN (10:1 wt. %) mixture to provide pseudo-hydrostatic conditions at high pressures and high temperatures, which was also served as an internal pressure maker. Pressures were calculated from Decker's equation of state for NaCl.[21] Uncertainties in the pressure are less than 0.2 GPa in the current pressure range. Temperatures were measured by a W/Re 26%–W/Re 5% thermocouple placed against the MgO cap next to the NaCl backing piece.

The P–T path for the current experiment is plotted in Fig. 1(b). The tungsten sample was initially compressed to the highest pressure of 11.2 GPa, followed by heating to the maximum temperature of 1073 K at a constant ram load to relax the nonhydrostatic stress and subsequent cooling to room temperature. The same procedure was repeated five times at progressively lower ram load. Data were collected along the cooling process during each cycle. Energy dispersive x-ray diffraction patterns were collected at the interface between the sample and NaCl with a fix 2θ (6.09°)

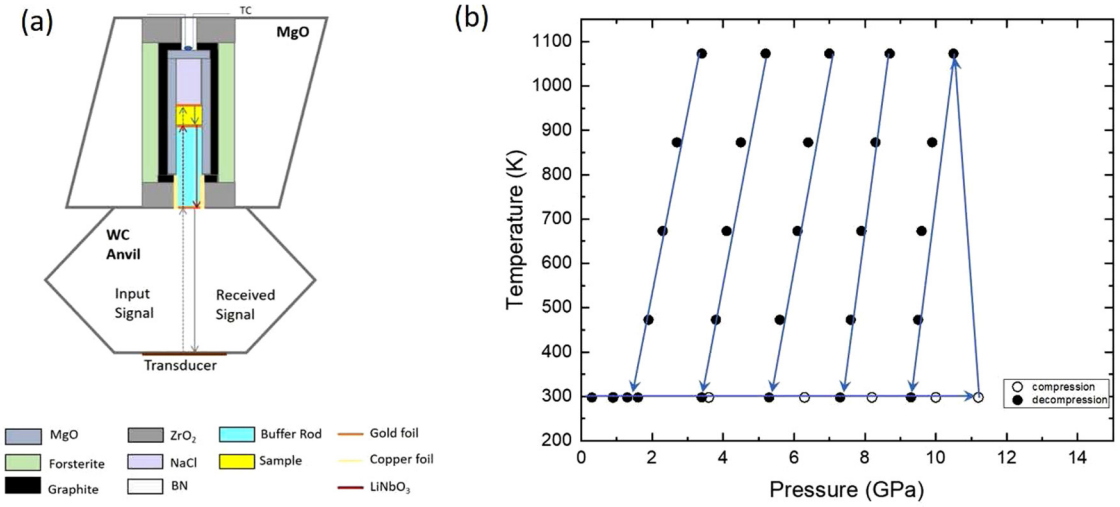

FIG. 1. (a) Schematic diagram of the cross section of the cell assembly. (b) Experimental pressure–temperature path. The open circles represent the data collecting upon cold compression, whereas the solid circles are data collecting at certain P–T conditions along cooling.

due to strong x-ray absorption of tungsten. The recorded diffraction profiles were analyzed using the software program PDIndexer[22] to obtain the lattice parameters and thus densities at high P–T conditions. The relative standard deviations in the unit cell volumes are typically less than 0.1%. P and S wave travel times were obtained using the pulse echo overlap (PEO) method with a resolution of 0.2 ns. Sample lengths were determined from the pixel profile using ImageJ[23] by analyzing the x-radiography images recorded by the charge-coupled device (CCD) camera with a resolution of 2 μm/pixel. The acoustic travel time measurements have a resolution of 0.2 ns,[20] resulting in an error less than $\pm$ 0.1% in the compressional (P) and shear (S) wave travel times for W. The propagated uncertainties in V_P and V_S were mainly from the uncertainty in the determination of sample length, which was ~0.5% in this study.

TABLE I. Lattice parameters and unit-cell volumes of tungsten at various P–T conditions.

Pressure (GPa)	Temperature (K)	a (Å)	V (Å^3)
Compression (before heating)			
0.9	298	3.1608(2)	31.579(7)
3.6	298	3.1518(2)	31.311(6)
6.3	298	3.1438(2)	31.072(7)
8.2	298	3.1373(3)	30.880(8)
10.0	298	3.1321(2)	30.726(7)
11.2	298	3.1283(2)	30.616(7)
Decompression (after heating)			
0.3	298	3.1638(5)	31.667(16)
0.9	298	3.1613(4)	31.593(11)
1.3	298	3.1608(4)	31.578(10)
1.6	298	3.1597(3)	31.546(10)
3.4	298	3.1532(2)	31.350(7)
5.3	298	3.1477(3)	31.187(16)
7.3	298	3.1411(3)	30.993(10)
9.3	298	3.1343(3)	30.791(10)
1.9	473	3.1600(4)	31.555(11)
3.8	473	3.1548(3)	31.398(6)
5.6	473	3.1485(3)	31.212(8)
7.6	473	3.1431(3)	31.050(8)
9.5	473	3.1373(5)	30.880(13)
2.3	673	3.1634(3)	31.658(9)
4.1	673	3.1565(3)	31.451(9)
6.1	673	3.1491(3)	31.231(10)
7.9	673	3.1442(3)	31.084(9)
9.6	673	3.1387(4)	30.921(12)
2.7	873	3.1639(4)	31.670(13)
4.5	873	3.1577(4)	31.484(11)
6.4	873	3.1520(4)	31.317(8)
8.3	873	3.1459(3)	31.135(10)
9.9	873	3.1408(3)	30.981(13)
3.4	1073	3.1663(4)	31.743(13)
5.2	1073	3.1582(6)	31.501(16)
7.0	1073	3.1534(4)	31.357(10)
8.7	1073	3.1487(6)	31.217(17)
10.5	1073	3.1435(3)	31.064(9)

RESULTS AND DISCUSSION

The unit cell volume of W obtained at ambient conditions in this experiment is $V_0 = 31.68(1)$ Å^3 and the lattice parameter $a = 3.1642(1)$ Å, which are in good agreement with previous studies varying from 31.68 to 31.72 Å.[15,17,18] The unit cell volumes and lattice parameters at all P–T conditions are listed in Table I. The unit cell volumes are plotted as a function of pressure and temperature in Fig. 2 and compared with previous studies. The results are consistent with those reported by Dewaele *et al.*[15] and Litasov *et al.*[17] within the current pressure and temperature range. To derive the thermoelastic properties, the observed P–V–T data are first fitted to a modified high-temperature Birch–Murnaghan equation of state truncated at the third order, given by[24]

$$P = \frac{3}{2}K_{T0}\left[\left(\frac{V_{T0}}{V}\right)^{\frac{7}{3}} - \left(\frac{V_{T0}}{V}\right)^{\frac{5}{3}}\right] \times \left\{1 + \frac{3}{4}(K'_{T0} - 4)\left[\left(\frac{V_{T0}}{V}\right)^{\frac{2}{3}} - 1\right]\right\}, \quad (1)$$

$$K_{T0} = K_{T0,298\ \mathrm{K}} + (T - 298)\left(\frac{\partial K_T}{\partial T}\right)_P, \quad (2)$$

where $K_{T0,298K}$ and K_{T0} denote isothermal bulk modulus at 298 K and any given temperature T. K'_{T0} and $\left(\frac{\partial K_T}{\partial T}\right)_P$ are the pressure and temperature derivatives of the bulk modulus, respectively. V_{T0} is the unit-cell volume at atmospheric pressure and temperature T,

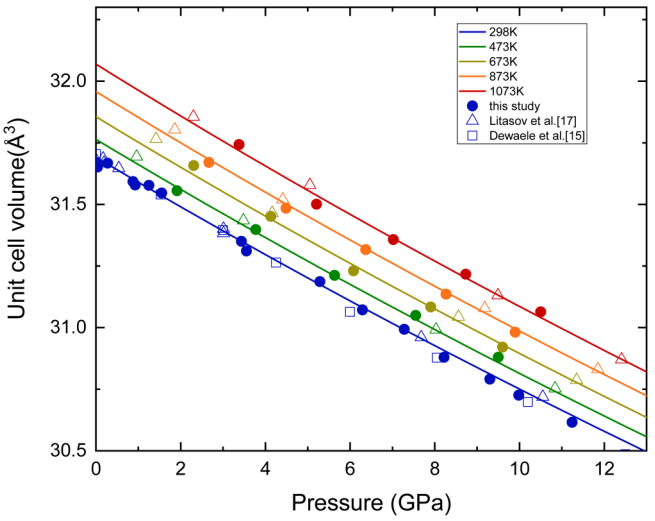

FIG. 2. Pressure–volume–temperature data of tungsten along isotherm. Solid circles are data from current experiments. Open squares are results from Litasov *et al.*[17] up to 1073 K, whereas open diamonds are data from Dewaele *et al.*[15] at room temperature. Solid lines represent the least-squares fit using a modified high-temperature Birch–Murnaghan equation of state at different temperatures.

which can be calculated by

$$V_{T0} = V_0 e^{\int \alpha dT}, \quad (3)$$

where V_0 is the unit cell volume at ambient conditions, and α is the volumetric thermal expansion at room pressure, commonly given in a form of $\alpha = a + bT$. To minimize the deviatoric stress effect, the unit cell volumes collected along cold compression before heating were excluded in the current fitting procedure. Using a least-squares fit with setting all parameters (unit cell volume at ambient conditions V_0, thermal expansion coefficient a and b, isothermal bulk modulus at room temperature K_{T0}, and its pressure and temperature derivatives (K'_{T0} and $\partial K_T/\partial T$) free, we obtain $V_0 = 31.691(1)$ Å^3, $K_{T0} = 310.3(1.5)$ GPa, $K'_{T0} = 4.4(3)$, $\partial K_T/\partial T = -0.0138(1)$ GPaK^{-1} $\alpha(0, T) = a + bT$, with $a = 1.02(27) \times 10^{-5}$ K^{-1} and $b = 7.39(3.2) \times 10^{-9}$ K^{-2}. The errors are one standard deviations of the least-squares fitting; uncertainties in the observed P–V–T data are not included for error estimation. As shown in Fig. 2, the derived thermoelastic parameters well reproduce the experimental P–V–T data. This bulk modulus of W agrees well with previous results of $K_{T0} = 307$ GPa at $K'_{T0} = 4.32$ by static compression experiments in a diamond anvil cell,[18] $K_{T0} = 317.5$ GPa at $K'_{T0} = 3.8$ by shock wave experiments,[25] and $K_{T0} = 308$ GPa at $K'_{T0} = 4.2$ by static compression experiments in a multi-anvil apparatus.[17] The volumetric thermal expansion from current study yields a value of 1.24×10^{-5} K^{-1} at room conditions, which is compatible with the range of 9.77×10^{-6} to 1.41×10^{-5} K^{-1} reported in previous studies by Dubrovinsky *et al.*,[26] Saxena *et al.*,[24] and Litasov *et al.*[17] (see details in Table II). The temperature derivative of bulk modulus at constant pressure $(\partial K_T/\partial T)_P = -0.0138(1)$ GPaK^{-1} falls in the range from −0.0132 to −0.0184 GPaK^{-1} reported by Litasov *et al.* using different fitting parameters.[17] This value is relatively smaller than those of neighbors of W in the Periodic Table, such as molybdenum Mo $(\partial K_T/\partial T)_P = -0.034(9)$ GPaK^{-1} by Zhao *et al.*[27] and niobium Nb $(\partial K_T/\partial T)_P = -0.064(7)$ GPaK^{-1} by Zou *et al.*[28] Based on thermodynamic equation $\left(\frac{\partial \alpha}{\partial P}\right)_T = \left(\frac{\partial K_T}{\partial T}\right)_P K_{T0}^{-2}$, the pressure derivative of the thermal expansion is determined to be $-1.44(1) \times 10^{-7}$ K^{-1}GPa^{-1}, in which the uncertainty is estimated from the error propagation of $(\partial K_T/\partial T)_P$ and ∂K_{T0}.

The Birch–Murnaghan EOS is based on the assumption that strain energy of a solid under hydrostatic compression can be expressed as a Taylor series in the finite Eulerian strain.[29] It is known that a low-order truncation of energy does not suffice to fit the experimental data under very high pressures.[30] At $V/V_0 < 0.6$, the Vinet EOS, derived from an empirical inter-atomic potential, is in much better agreement with experimental data for metals, dielectrics, and ionic solids, if no phase transition is observed.[31] The Vinet formulation of EOS is[2]

$$P = 3K_0 x^{-2}(1-x)\exp[(1.5K'_o - 1.5)(1-x)], \quad (4)$$

where $x = (V/V_0)^{\frac{1}{3}}$ is simply the linear compression. In order to fit all P–V–T data, temperature effects need to be introduced in

TABLE II. Thermoelastic parameters of tungsten derived using different approaches compared with previous studies. (The bold values have been fixed during the fitting procedure.)

Reference	This study				1[a]		2[b]	3[c]	4[d]
	HTBM[e]	Vinet[f]	TP[g]	FS[h]	HTBM[e]	MGD[i]	HTBM[e]	Ultrasonic	HTBM[e]
V_0(Å^3)	31.691(1)	31.691(1)	31.690(1)	31.691	31.71	31.698			31.69(2)
$\mathbf{K_{T0}}$(GPa)	310.3(1.5)	310.3(1.5)	310.4(1.5)	312.4(2.5)	308	307	311.6	308.6	304(2)
K_{T0}'	4.4(3)	4.5(3)	4	4.4(9)	4.2	4.25	3.5	4.32	4.09(33)
$(\partial K_T/\partial T)_P$(GPa K^{-1})	−0.0138(1)	−0.0139(1)	−0.0135(1)	−0.0155(15)	−0.0184	…	−0.0188		
G_0(GPa)	…	…	…	162.4(9)	…	…		160	
G_0'	…	…	…	1.8(1)	…	…		1.52	
$\partial G/\partial T$(GPa K^{-1})	…	…	…	−0.0175(9)	…	…		…	
a(×10^{-5} K^{-1})	1.02(27)	1.02(28)	…	1.02	1.35	…	0.94	…	1.37
B(×10^{-8} K^{-2})	0.739(3.2)	0.737(3.2)	…	0.7	0.21	…	0.55	…	−0.074
$\alpha_{298\,K}$(×10^{-5} K^{-1})	1.24	1.24	…	1.23	1.41	…	1.10	1.35	0.112*
γ_0	…	…	1.79	…	1.72	1.81		1.65	
$(\partial\alpha/\partial P)_T$(×10^{-7} K^{-1})	−1.44(1)	−1.44(1)	−1.40(1)	…	…	…	…	…	
αK_T(GPa K^{-1})	…	…	0.0047	…	…	…	…	…	

[a]Litasov *et al.* (2013),[17] W powder , up to 33.5 GPa and 1673 K.
[b]Saxena *et al.* (1990),[24] data synthesis.
[c]Katahara *et al.* (1979),[10] single crystal W, up to 0.5 GPa and 300 K.
[d]Dubrovinsky *et al.* (2010),[16] single crystal W, up to 46.6 GPa and 2100 K. *Thermal expansion is given as $\alpha(0, T) = a + bT - c/T^2$, where c=1.098(3).
[e]High-temperature Birch–Murnaghan EOS.
[f]Vinet EOS.
[g]Thermal pressure approach.
[h]Finite strain EOS.
[i]Mie–Grüneisen–Debye EOS.

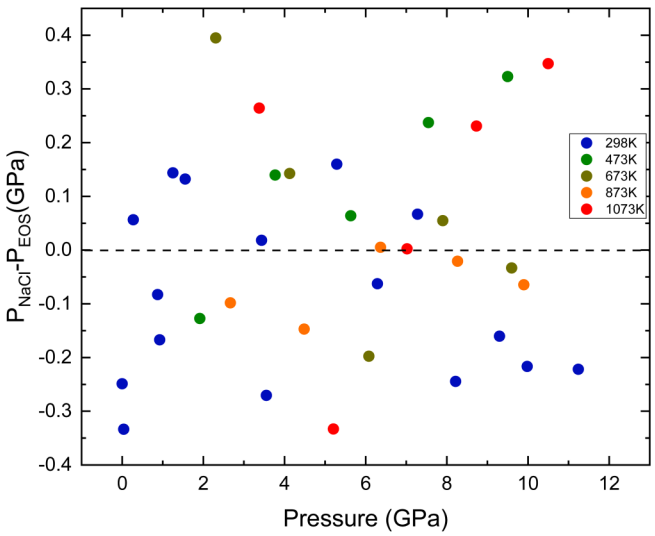

FIG. 3. Differences between pressures calculated using EOS of NaCl and the Vinet EOS along all isotherms.

the Vinet EOS. Similar modifications as to that for the high-temperature Birch–Murnaghan EOS are applied here, i.e., $x = (V_{PT}/V_{T0})^{\frac{1}{3}}$ and K_0 is replaced with $K_T = K_{T0} + \left(\frac{\partial K}{\partial T}\right)(T - 298)$. High-order temperature derivatives have been ignored due to the limited P–T range and a small volumetric compression of tungsten reached in the current experiments. The derived parameters from the Vinet EOS are essentially the same as those derived from the Birch–Murnaghan EOS within their mutual uncertainties (see Table II). Both EOSs can reproduce the P–V–T data well in current P–T ranges. The goodness of the EOS fit is evaluated by the differences in pressure between the experimental values derived from the EOS of NaCl and those calculated using Vinet EOS, and the results for all isotherms are shown in Fig. 3. We note that the deviations are distributed evenly within the pressure range, and the uncertainties in pressures are within 0.4 GPa.

Another way to analyze the P–V–T data is the thermal pressure approach based on the Mie–Grüneisen theory.[32,33] The method is useful for determining $(\partial K_T/\partial T)_V$, the temperature derivative for bulk modulus at a constant volume, which is experimentally difficult to measure. In contrast to the high-temperature Birch–Murnaghan EOS approach which involves first heating V (0, 298 K) at ambient conditions to high temperature T along $P = 0$ and then compressing the expanded volume $V(0, T)$ along the isotherm to reach the measured $V(P, T)$, the thermal pressure approach first compresses the ambient $V(0, 298\,K)$ to high pressure P along $T = 298$ K and then heats it up to temperature T at constant volume to reach $V(P, T)$. As expressed in Eq. (5), the thermal pressure P_{th} at any temperature above 298 K is calculated by subtracting the pressure at volume V and at 298 K from the pressure measured at the same V and at a given temperature T,[32,34]

$$P_{th} = P(V, T) - P(V, 298) = \int_{298\,k}^{T} (\partial P/\partial T)_V dT = \alpha K_T (V_{298}, T) + [(\partial K_T/\partial T)_V \ln (V_{298}/V)](T - 298). \quad (5)$$

Following this definition, thermal pressures for W as a function of temperature and unit cell volume are plotted in Fig. 4. As shown in Fig. 4(a), the thermal pressure increases almost linearly with temperature. A least-squares fit of thermal pressure values from the whole P–V–T dataset to Eq. (5) yields $\alpha K_T(V_{298}, T) = 0.0046$ and $\left(\frac{\partial K_T}{\partial T}\right)_V = 0.0050$ GPa K^{-1}. If considering the uncertainty in the fitting, the value of $\left(\frac{\partial K_T}{\partial T}\right)_V$ is close to zero, which is consistent with the linear fit result of the thermal pressure vs temperature $\alpha K_T(V_{298}, T) = 0.0047$ GPaK^{-1} in Fig. 4(a). From the well-known thermodynamic identity

$$(\partial K_T/\partial T)_V = (\partial K_T/\partial T)_P + (\partial K_T/\partial P)_T \alpha K_T(V_{298}, T), \quad (6)$$

we obtain $(\partial K_T/\partial T)_P = -0.0135$ GPa K^{-1}, which is comparable to the value of -0.0138 GPa K^{-1} derived from Eq. (2). $\left(\frac{\partial \alpha}{\partial P}\right)_T$ is determined to be $-1.40(1) \times 10^{-7}$ K^{-1}GPa^{-1}, which is in excellent agreement with the result of $-1.44(1) \times 10^{-7}$ K^{-1}GPa^{-1} from the high-temperature Birch–Murnaghan EOS. With determined αK_T, the thermal Grüneisen parameter can be derived using the expression

$$\gamma_{th} = \frac{\alpha K_T}{\rho C_V}, \quad (7)$$

with $\rho_0 = 19.26$ g/cm^3 and the isochoric heat capacity $C_V = 13.1$ J/mol K,[14] the thermal Grüneisen parameter of tungsten yields $\gamma_{th} = 1.82$, which is within the range of 1.53–2.20 reported in previous studies (e.g., Refs. 10, 14, and 17), but in a closer agreement with the value of 1.81 by Litasov *et al.*[17]

The compressional (P) and shear (S) wave velocities $\left(V_{(P,S)} = \frac{l}{t_{(P,S)}}\right)$ on decompression along cooling after peak pressure and temperature are plotted in Fig. 5 and compared with previous ultrasonic measurements at room temperature by Qi. *et al.*[13] Both P and S wave velocities along 298 K isotherm show marginal agreement with previous results within their mutual uncertainties. The elastic longitudinal ($L = \rho V_P^2 = K_S + 4G/3$) and shear ($G = \rho V_S^2$) moduli at all pressure and temperature conditions are calculated from the velocity and density data (see Table III) and plotted as a function of pressure and temperature in Fig. 6. Both the velocities and the elastic moduli increase with increasing

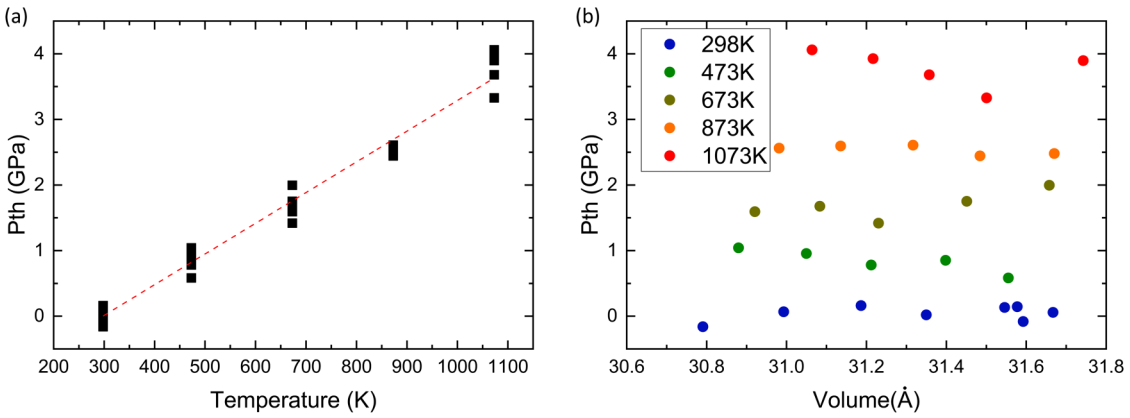

FIG. 4. (a) Thermal pressures of tungsten as a function of temperature. Red dashed line is the linear fit result. (b) The spread of the data points at a given temperature corresponding to the thermal pressures at given volumes.

pressure and decrease with increasing temperature. Similar pressure dependence of velocities and elastic moduli can be found at different isotherms. Assuming linear pressure and temperature dependences for K_S and G, K_S, and G are first fitted simultaneously to the following equations:

$$K_S = K_{S0} + \frac{\partial K_S}{\partial P}(P - P_0) + \frac{\partial K_S}{\partial T}(T - T_0), \tag{8}$$

$$G = G_0 + \frac{\partial G}{\partial P}(P - P_0) + \frac{\partial G}{\partial T}(T - T_0). \tag{9}$$

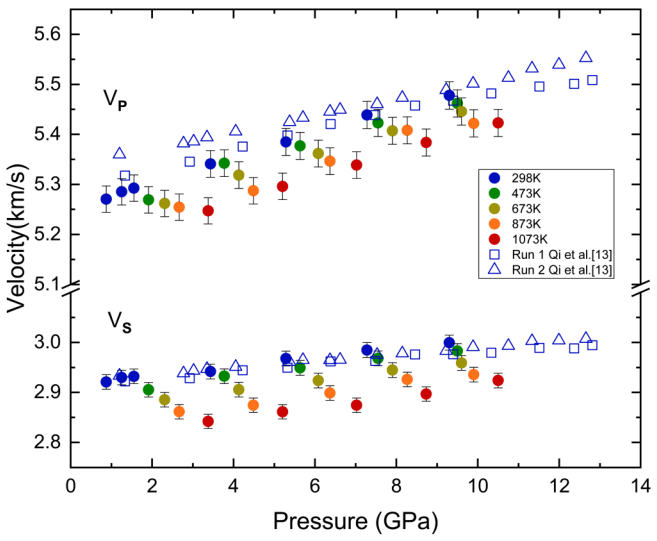

FIG. 5. Compressional and shear wave velocities of tungsten at high pressures and high temperatures.

We obtain $K_{S0} = 313.7$ GPa, $K_{S0}' = 4.7$, $\partial K_S/\partial T = -0.0086$ GPa K^{-1}, $G_0 = 163.5$ GPa, $G' = 1.7$, $\partial G/\partial T = -0.0176$ GPa K^{-1}. However, this method is lack of clear physical meaning. Experimental errors in pressure and temperature may greatly affect the fitting results. We then used the finite strain approach to fit all data along decompression. The equations are given by[35]

$$\rho V_P^2 = (1 - 2f)^{\frac{5}{2}}(L_1 + L_2 f), \tag{10}$$

$$\rho V_S^2 = (1 - 2f)^{\frac{5}{2}}(M_1 + M_2 f), \tag{11}$$

where $f = \left[1 - \left(\frac{V_0}{V}\right)^{2/3}\right]/2$ is the Eulerian strain. With derived L_1, L_2, M_1, and M_2, the adiabatic bulk (K_{s0}) and shear modulus (G_0), as well as their isothermal pressure derivative (K_{s0}' and G_0'), can be calculated using the following equations:

$$K_{S0} = L_1 - \frac{4}{3}M_1, \tag{12}$$

$$G_0 = M_1, \tag{13}$$

$$K_{S0}' = \frac{5L_1 - L_2}{3K_{S0}} - \frac{4G_0'}{3}, \tag{14}$$

$$G_0' = \frac{5M_1 - M_2}{3K_{S0}}. \tag{15}$$

The temperature derivatives are determined from fitting all data at high P–T conditions using Eqs. (10)–(15) by assuming all temperatures to be raised along separate adiabatic compression with different foot temperature at zero pressure. Details about this fitting procedure can be found in Ref. 36. Using this approach with V_0 fixed at 31.691 Å^3 and $\gamma_0 = 1.79$ from our previous calculations, $q_0 = 0.71$ from Litasov *et al.*,[17] we obtain $K_{S0} = 314.5(2.5)$ GPa, $K_{S0}' = 4.45(9)$, $(\partial K_S/\partial T)_P = -0.0076(6)$ GPa K^{-1}, $G_0 = 162.4(9)$ GPa, $G_0' = 1.8(1)$, $(\partial G/\partial T)_P = -0.0175(9)$ GPa K^{-1}, and $\alpha = a + bT$

TABLE III. Experimental data for tungsten at high pressures and high temperatures.

P (GPa)	T (K)	$2T_P$ (μs)	$2T_S$ (μs)	Length (mm)	Density (g/cm^3)	V_P (km/s)	V_S (km/s)	K_S (GPa)	G (GPa)	L (GPa)
0.9	298	0.2884(2)	0.5204(2)	0.760(2)	19.33(1)	5.27(3)	2.92(1)	317.1(5)	164.9(3)	537.3(8)
1.3	298	0.2876(2)	0.5188(2)	0.760(2)	19.34(1)	5.29(3)	2.93(1)	318.9(5)	166.0(3)	540.4(8)
1.6	298	0.2872(2)	0.5184(2)	0.760(2)	19.36(1)	5.29(3)	2.93(1)	320.4(5)	166.5(3)	542.1(8)
3.4	298	0.2820(2)	0.5120(2)	0.753(2)	19.48(1)	5.34(3)	2.94(1)	331.0(5)	168.6(5)	563.4(8)
5.3	298	0.2780(2)	0.5044(2)	0.748(2)	19.58(1)	5.38(3)	2.97(1)	337.9(5)	172.5(5)	580.8(9)
7.3	298	0.2744(2)	0.5000(2)	0.746(2)	19.71(1)	5.44(3)	2.98(1)	348.8(5)	175.6(5)	597.3(9)
9.3	298	0.2716(2)	0.4960(2)	0.744(2)	19.84(1)	5.48(3)	3.00(1)	357.2(5)	178.5(5)	611.1(9)
1.9	473	0.2876(2)	0.5216(2)	0.758(2)	19.36(1)	5.27(3)	2.91(1)	319.5(5)	163.4(5)	540.5(8)
3.8	473	0.2828(2)	0.5152(2)	0.755(2)	19.45(1)	5.34(3)	2.93(1)	332.1(5)	167.3(5)	560.0(8)
5.6	473	0.2784(2)	0.5076(2)	0.748(2)	19.57(1)	5.38(3)	2.95(1)	338.8(5)	170.2(5)	578.9(9)
7.6	473	0.2752(2)	0.5028(2)	0.746(2)	19.67(1)	5.42(3)	2.97(1)	347.4(5)	173.3(5)	593.5(9)
9.5	473	0.2724(2)	0.4988(2)	0.744(2)	19.78(1)	5.46(3)	2.98(1)	355.4(5)	176.0(5)	606.9(9)
2.3	673	0.2880(2)	0.5252(2)	0.758(2)	19.29(1)	5.26(3)	2.89(1)	320.0(5)	160.6(5)	538.4(8)
4.1	673	0.2832(2)	0.5184(2)	0.753(2)	19.42(1)	5.32(3)	2.91(1)	330.7(5)	163.9(5)	558.1(8)
6.1	673	0.2792(2)	0.5120(2)	0.748(2)	19.56(1)	5.36(3)	2.92(1)	339.3(5)	167.2(5)	575.5(9)
7.9	673	0.2760(2)	0.5068(2)	0.746(2)	19.65(1)	5.41(3)	2.94(1)	347.3(5)	170.4(5)	589.9(9)
9.6	673	0.2732(2)	0.5028(2)	0.744(2)	19.75(1)	5.45(3)	2.96(1)	355.2(5)	172.9(5)	603.1(9)
2.7	873	0.2884(2)	0.5296(2)	0.758(2)	19.29(1)	5.25(3)	2.86(1)	321.9(5)	157.9(5)	536.9(8)
4.5	873	0.2840(2)	0.5224(2)	0.751(2)	19.40(1)	5.29(3)	2.87(1)	328.6(5)	160.3(5)	554.7(8)
6.4	873	0.2800(2)	0.5164(2)	0.748(2)	19.50(1)	5.35(3)	2.90(1)	338.9(5)	163.9(5)	571.7(9)
8.3	873	0.2768(2)	0.5116(2)	0.748(2)	19.62(1)	5.41(3)	2.93(1)	349.8(5)	168.0(5)	586.1(9)
9.9	873	0.2744(2)	0.5068(2)	0.744(2)	19.71(1)	5.42(3)	2.94(1)	353.0(5)	169.9(5)	597.4(9)
3.4	1073	0.2888(2)	0.5332(2)	0.758(2)	19.24(1)	5.25(3)	2.84(1)	322.5(5)	155.4(5)	535.0(8)
5.2	1073	0.2844(2)	0.5264(2)	0.753(2)	19.39(1)	5.30(3)	2.86(1)	332.2(5)	158.7(5)	553.1(8)
7	1073	0.2804(2)	0.5208(2)	0.748(2)	19.48(1)	5.34(3)	2.87(1)	340.6(5)	160.9(5)	569.8(9)
8.7	1073	0.2772(2)	0.5152(2)	0.746(2)	19.57(1)	5.38(3)	2.90(1)	348.2(5)	164.2(5)	583.9(9)
10.5	1073	0.2752(2)	0.5104(2)	0.746(2)	19.66(1)	5.42(3)	2.92(1)	354.1(5)	168.1(5)	593.4(9)

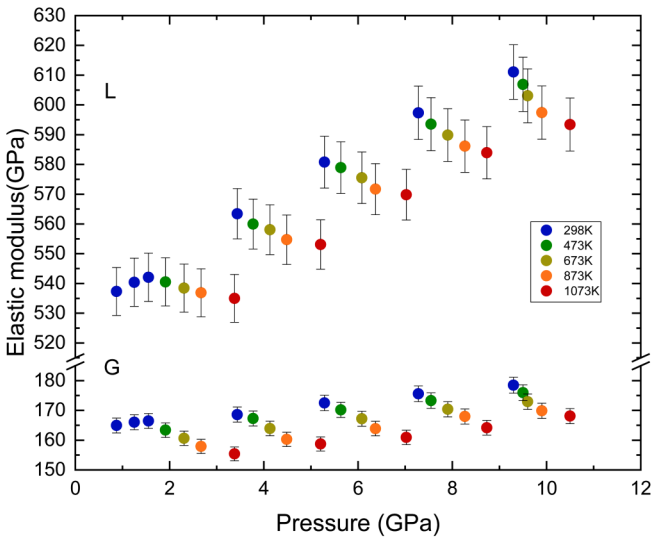

FIG. 6. Longitudinal and shear moduli of tungsten at high pressures and high temperatures.

with $a = 1.02 \times 10^{-5}\,\mathrm{K}^{-1}$, $b = 7.00 \times 10^{-9}\,\mathrm{K}^{-2}$. The determined thermal expansion at 298 K is $1.23 \times 10^{-5}\,\mathrm{K}^{-1}$, which is in excellent agreement with that derived from the high-temperature Birch–Murnaghan EOS. The adiabatic parameters K_{S0}, K_{S0}' and $(\partial K_S/\partial T)_P$ can be converted to the isothermal values using the following thermodynamic relations: $K_T = K_S/(1+\alpha\gamma T)$, $K_{T0}' \cong (1+\alpha\gamma T)^{-1}[K_{S0}' - \gamma T/K_T(\partial K_S/\partial T)_P]$, $(\partial K_T/\partial T)_P \cong (\partial K_S/\partial T)_P/(1+\alpha\gamma T) - K_S/(1+\alpha\gamma T)^2[\alpha\gamma + (\partial\alpha/\partial T)\gamma T]$,[37] yielding $K_{T0} = 312.4(2.5)$ GPa, $K_{T0}' = 4.4(9)$ and $(\partial K_T/\partial T)_P = -0.0155(15)$ GPa K^{-1}, which is consistent within uncertainties with results using the high-temperature Birch–Murnaghan EOS and the thermal pressure approach (see Table II). A recent ultrasonic study on W at high pressures and room temperature by Qi *et al.*[13] reported $K_{S0} = 325.9$ (4.8) GPa, $K_{S0}' = 3.65(5)$, $G_0 = 164.1(2.5)$ GPa and $G_0' = 1.28(2)$. The shear modulus shows good agreement with current study within the uncertainties, but the bulk modulus is ~3.6% higher than the current result. The discrepancies may be attributed to a strong trade-off between K_{S0} and K_{S0}' which are constrained simultaneously by fitting to the EOS. To reduce uncertainties in K_0', larger datasets and wider pressure ranges are still needed.[38] Our current experiment offers the opportunity to directly evaluate the sound velocities and elastic moduli of tungsten at simultaneous high pressure and high temperature conditions. Moreover, the

finite strain method has the advantage of minimizing or eliminating the uncertainties resulting from errors in pressure measurement, thus the derived thermoelastic properties are not affected by the choice or accuracy of pressure scale.

With derived P and S wave velocities at room conditions [$V_P = 5.25(3)$ km/s $V_S = 2.91(1)$ km/s], Debye temperature θ_D can be calculated using the equation

$$\theta_D = \left(\frac{h}{k_B}\right)\left(\frac{3n}{4\pi}\right)^{1/3}\left(\frac{N_A\rho}{M}\right)^{1/3}\left(\frac{2}{3V_S^2}+\frac{1}{3V_P^2}\right)^{-1/3},$$

where h is Planck's constant, k_B is Boltzmann's constant, N_A is Avogadro's number, M is the molecular weight, and n is the number of atoms in the molecule. The derived result is $\theta_D = 383.4$ K, which is in excellent agreement with the value of 384.4 K by Bolef *et al.*[14] and Featherston *et al.*[12] The present P–V–T data have also been analyzed using the Mie–Grüneisen–Debye (MGD) EOS, which is another widely used and soundly based in the most fundamental concepts of lattice dynamics. The pressure at a given volume and temperature is expressed as[34]

$$P(V,\ T) = P(V,\ T_0) + \Delta P_{th}, \tag{16}$$

$$\Delta P_{th} = \frac{\gamma(V)}{V}[E_{th}(V,\ T) - E_{th}(V,\ T_0)], \tag{17}$$

where is $P(V,\ T_0)$ from taken from Eq. (1) and the thermal free energy E_{th} is calculated from the Debye model as described below,

$$E_{th} = \frac{9nRT}{(\theta/T)^3}\int_0^{\theta/T}\frac{x^3}{e^x-1}dx, \tag{18}$$

$$\theta = \theta_0 \exp\left(\frac{\gamma_0-\gamma}{q}\right), \tag{19}$$

$$\gamma = \gamma_0\left(\frac{V}{V_0}\right)^q, \tag{20}$$

where n is the number of atoms per formula unit, R is the gas content, θ is the Debye temperature depending on volume, γ_0 and θ_0 are the Grüneisen parameter and Debye temperature at V_0, respectively, and $q = (dln\gamma/dlnV)$. As the derived Debye temperature $\theta_0 = 383.4$ K, this value is fixed in our calculations. Using the EosFit7 program,[39] fitting to the current data yielded the Grüneisen parameter $\gamma_0 = 1.81(6)$ and its volume dependence $q = 0.3$, which is in great agreement with aforementioned $\gamma_{th} = 1.82$ by the thermal pressure approach. It is also found that the derived Grüneisen parameter is almost unaffected ($\gamma_0 = 1.81$–1.84) by varying the value of q from 0.3 to 1.5, which is common for metals and minerals.[34,40]

CONCLUSION

In summary, we have measured the compressional and shear wave velocities of polycrystalline tungsten up to 10.5 GPa and 1073 K using ultrasonic interferometry in conjunction with synchrotron x-ray diffraction and x-radiography techniques. Thermoelastic properties have been derived using the P–V–T dataset by different approaches, namely, high-temperature Birch–Murnaghan EOS, the Vinet formalism of EOS, thermal pressure approach, the finite strain method and Mie–Grüneisen–Debye EOS. The results are in good agreement with each other, which indicates the self-consistency of the whole dataset. The temperature derivate of shear modulus [$(\partial G/\partial T)_P = -0.0175$ GPa K^{-1}] and the pressure derivate of thermal expansion of tungsten ($\partial\alpha/\partial P = -1.44 \times 10^{-7}$ K^{-1}GPa^{-1}) are obtained for the first time. The present measurements provide a complete and self-consistent dataset for the thermoelastic properties of tungsten. These results offer important reference data to improve the theoretical modeling of the thermodynamic properties of crystalline solids with quasiharmonic approximation.

AUTHORS' CONTRIBUTIONS

All authors contributed equally to this work.

ACKNOWLEDGMENTS

The authors would like to thank Yanbin Wang and Tony Yu for technical support at 13-ID-D beamline of the Advanced Photon Source, Argonne National Laboratory. The authors are also thankful to Robert Liebermann, David Welch, and Sibo Chen for valuable discussions. This project is supported by DOE/NNSA (No. DE-NA0003886). GeoSoilEnviroCARS is supported by the National Science Foundation-Earth Sciences (No. EAR-1634415) and Department of Energy-GeoSciences (No. DE-FG02-94ER14466). This research used resources of the Advanced Photon Source, a U.S. Department of Energy (DOE) Office of Science User Facility operated for the DOE Office of Science by Argonne National Laboratory under Contract No. DE-AC02-06CH11357.

DATA AVAILABILITY

The data that support the findings of this study are available within the article.

REFERENCES

[1]F. Birch, "Finite strain isotherm and velocities for single-crystal and polycrystalline NaCl at high pressures and 300 K," J. Geophys. Res. Solid Earth **83**(B3), 1257–1268, https://doi.org/10.1029/JB083iB03p01257 (1978).
[2]P. Vinet, J. Ferrante, J. H. Rose, and J. R. Smith, "Compressibility of solids," J. Geophys. Res.: Solid Earth **92**(B9), 9319–9325, https://doi.org/10.1029/JB092iB09p09319 (1987).
[3]S. M. Dorfman, V. B. Prakapenka, Y. Meng, and T. S. Duffy, "Intercomparison of pressure standards (Au, Pt, Mo, MgO, NaCl and Ne) to 2.5 Mbar," J. Geophys. Res. Solid Earth **117**, B08210, https://doi.org/10.1029/2012JB009292 (2012).
[4]A. Dewaele, P. Loubeyre, F. Occelli, M. Mezouar, P. I. Dorogokupets, and M. Torrent, "Quasihydrostatic equation of state of iron above 2 Mbar," Phys. Rev. Lett. **97**(21), 215504 (2006).
[5]E. Lassner and W. D. Schubert, *The Element Tungsten* (Springer, Tungsten, 1999), pp. 1–59.
[6]S. Xiang, F. Xi, Y. Bi, J. A. Xu, H. Geng, L. Cai, F. Jing, and J. Liu, "*Ab initio* thermodynamics beyond the quasiharmonic approximation: W as a prototype," Phys. Rev. B **81**(1), 014301 (2010).
[7]Y. Wang, D. Chen, and X. Zhang, "Calculated equation of state of Al, Cu, Ta, Mo, and W to 1000 GPa," Phys. Rev. Lett. **84**(15), 3220 (2000).

[8]J. A. Moriarty, "Ultrahigh-pressure structural phase transitions in Cr, Mo, and W," Phys. Rev. B **45**(5), 2004 (1992).
[9]H. Y. Zhang, Z. W. Niu, L. C. Cai, X. R. Chen, and F. Xi, "*Ab initio* dynamical stability of tungsten at high pressures and high temperatures," Comput. Mater. Sci. **144**, 32–35 (2018).
[10]K. Katahara, M. H. Manghnani, and E. S. Fisher, "Pressure derivatives of the elastic moduli of BCC Ti-V-Cr, Nb-Mo and Ta-W alloys," J. Phys. F Met. Phys. **9**(5), 773 (1979).
[11]D. I. Bolef and J. De Klerk, "Elastic constants of single-crystal Mo and W between 77 and 500 K," J. Appl. Phys. **33**(7), 2311–2314 (1962).
[12]F. H. Featherston and J. R. Neighbours, "Elastic constants of tantalum, tungsten, and molybdenum," Phys. Rev. **130**(4), 1324 (1963).
[13]X. Qi, N. Cai, T. Chen, S. Wang, and B. Li, "Experimental and theoretical studies on the elasticity of tungsten to 13 GPa," J. Appl. Phys. **124**(7), 075902 (2018).
[14]R. S. Hixson and J. N. Fritz, "Shock compression of tungsten and molybdenum," J. Appl. Phys. **71**(4), 1721–1728 (1992).
[15]A. Dewaele, P. Loubeyre, and M. Mezouar, "Equations of state of six metals above 94 GPa," Phys. Rev. B **70**(9), 094112 (2004).
[16]L. Dubrovinsky, T. Boffa-Ballaran, K. Glazyrin, A. Kurnosov, D. Frost, M. Merlini, M. Hanfland, V. B. Prakapenka, P. Schouwink, T. Pippinger, and N. Dubrovinskaia, "Single-crystal X-ray diffraction at megabar pressures and temperatures of thousands of degrees," High Pressure Res. **30**(4), 620–633 (2010).
[17]K. D. Litasov, P. N. Gavryushkin, P. I. Dorogokupets, I. S. Sharygin, A. Shatskiy, Y. Fei, S. V. Rashchenko, Y. V. Seryotkin, Y. Higo, K. Funakoshi, and E. Ohtani, "Thermal equation of state to 33.5 GPa and 1673 K and thermodynamic properties of tungsten," J. Appl. Phys. **113**(13), 133505 (2013).
[18]L. C. Ming and M. H. Manghnani, "Isothermal compression of bcc transition metals to 100 kbar," J. Appl. Phys. **49**(1), 208–212 (1978).
[19]G. D. Gwanmesia and R. C. Liebermann, "Polycrystals of high-pressure phases of mantle minerals: Hot-pressing and characterization of physical properties," High-Pressure Res. Appl. Earth Planet. Sci. **135**, 117 (1992).
[20]B. Li and R. C. Liebermann, "Study of the earth's interior using measurements of sound velocities in minerals by ultrasonic interferometry," Phys. Earth Planet. Inter. **233**, 135–153 (2014).
[21]D. L. Decker, "High-pressure equation of state for NaCl, KCl, and CsCl," J. Appl. Phys. **42**(8), 3239–3244 (1971).
[22]Y. Seto, "Development of a software suite on X-ray diffraction experiments," Rev. High Pressure Sci. Technol. **20**, 269–276 (2010).
[23]W. S. Rasband, ImageJ, Bethesda, MD, 1997.
[24]S. K. Saxena and J. Zhang, "Thermochemical and pressure-volume-temperature systematics of data on solids, examples: Tungsten and MgO," Phys. Chem. Miner. **17**(1), 45–51 (1990).
[25]T. Mashimo, X. Liu, M. Kodama, E. Zaretsky, M. Katayama, and K. Nagayama, "Effect of shear strength on Hugoniot-compression curve and the equation of state of tungsten (W)," J. Appl. Phys. **119**(3), 035904 (2016).
[26]L. S. Dubrovinsky and S. K. Saxena, "Thermal expansion of periclase (MgO) and tungsten (W) to melting temperatures," Phys. Chem. Miner. **24**(8), 547–550 (1997).
[27]Y. Zhao, A. C. Lawson, J. Zhang, B. I. Bennett, and R. B. Von Dreele, "Thermoelastic equation of state of molybdenum," Phys. Rev. B **62**(13), 8766 (2000).
[28]Y. Zou, Y. Li, H. Chen, D. Welch, Y. Zhao, and B. Li, "Thermoelasticity and anomalies in the pressure dependence of phonon velocities in niobium," Appl. Phys. Lett. **112**(1), 011901 (2018).
[29]F. Birch, "Elasticity and constitution of the earth's interior," J. Geophys. Res. **57**(2), 227–286, https://doi.org/10.1029/JZ057i002p00227 (1952).
[30]R. E. Cohen, O. Gülseren, and R. J. Hemley, "Accuracy of equation-of-state formulations," Am. Mineral. **85**(2), 338–344 (2000).
[31]J. Hama and K. Suito, "The search for a universal equation of state correct up to very high pressures," J. Phys. Condens. Matter **8**(1), 67 (1996).
[32]O. L. Anderson, "A universal thermal equation-of-state," J. Geodyn. **1**(2), 185–214 (1984).
[33]O. L. Anderson and P. A. Lee, *Equations of State of Solids for Geophysics and Ceramic Science* (Oxford University Press on Demand, 1995).
[34]I. Jackson and S. M. Rigden, "Analysis of P-V-T data: Constraints on the thermoelastic properties of high-pressure minerals," Phys. Earth Planet. Inter. **96**(2–3), 85–112 (1996).
[35]G. F. Davies and A. M. Dziewonski, "Homogeneity and constitution of the earth's lower mantle and outer core," Phys. Earth Planet. Inter. **10**(4), 336–343 (1975).
[36]B. Li and J. Zhang, "Pressure and temperature dependence of elastic wave velocity of $MgSiO_3$ perovskite and the composition of the lower mantle," Phys. Earth Planet. Inter. **151**(1), 143–154 (2005).
[37]S. Speziale and T. S. Duffy, "Single-crystal elastic constants of fluorite (CaF_2) to 9.3 GPa," Phys. Chem. Miner. **29**(7), 465–472 (2002).
[38]Z. Jing and S. I. Karato, "Compositional effect on the pressure derivatives of bulk modulus of silicate melts," Earth Planet. Sci. Lett. **272**(1–2), 429–436 (2008).
[39]J. Gonzalez-Platas, M. Alvaro, F. Nestola, and R. Angel, "EosFit7-GUI: A new graphical user interface for equation of state calculations, analyses and teaching," J. Appl. Crystallogr. **49**(4), 1377–1382 (2016).
[40]T. S. Duffy and T. J. Ahrens, "Compressional sound velocity, equation of state, and constitutive response of shock-compressed magnesium oxide," J. Geophys. Res. Solid Earth **100**(B1), 529–542, https://doi.org/10.1029/94JB02065 (1995).